

Modeling of 3-Level Buck Converters in Discontinuous Conduction Mode for Stand-by Mode Power Supply

Yoshitaka Yamauchi, Toru Sai, Takayasu Sakurai, and Makoto Takamiya
University of Tokyo, Tokyo, Japan

Abstract— A 3-level buck converter in the discontinuous conduction mode (DCM) is a key circuit for integrated voltage regulators to achieve high efficiency at a light load in the stand-by mode operation of microprocessors. In this paper, fundamental circuit characteristics including the conversion ratio and transfer function are derived for the first time, enabling the design of controllers for 3-level buck converters in the DCM. The derived transfer function is verified by time-domain small-signal-injection simulation. Similar to conventional 2-level buck converters, 3-level buck converters in the DCM have a first-order lag transfer function, while 3-level buck converters in the continuous conduction mode (CCM) have a second-order lag transfer function, suggesting that different controllers are required for the DCM and CCM.

I. INTRODUCTION

To enable the energy-efficient operation of many-core microprocessors, fine-grained per-core dynamic voltage scaling is required. As the number of cores increases, the required number of power supply voltages (V_{DD}) also increases. Integrated voltage regulators (IVRs) are a means of generating multiple V_{DD} on a chip, because increasing the number of off-chip voltage regulators is not practical. The key requirements of IVRs are a high power conversion efficiency (η) and a small form factor.

As shown in Fig. 1, a 3-level buck converter [1-6] combining a cascode 2-level buck converter [7] and a 1/2 switched capacitor DC-DC converter is a key circuit for IVRs, because the 3-level buck converter has a smaller inductance and faster transient response than the conventional 2-level buck converter at fixed ripples [2,5,6]. A fully integrated 3-level buck converter in the continuous conduction mode (CCM) delivering a current of 150mA with η of 72% for the active mode operation of microprocessors has been reported [2]. The converter, however, cannot be applied to the stand-by mode operation of microprocessors because η is low at a light load (e.g., < 1mA) owing to the CCM. In IVRs for energy-efficient microprocessors, a high η in the stand-by mode as well as the active mode is required. To achieve a high η at a light load, discontinuous conduction mode (DCM) operation is required. However, there have been very few publications of 3-level buck converters in the DCM [4], although a detailed analysis of a 3-level buck converter in the CCM was reported in [5,6]. Reference [4] does not include an analysis on the fundamental circuit characteristics of a 3-level buck converter in the DCM, meaning that it is not yet clarify to design controllers.

To solve this problem, in this paper, fundamental circuit characteristics including the conversion ratio and transfer

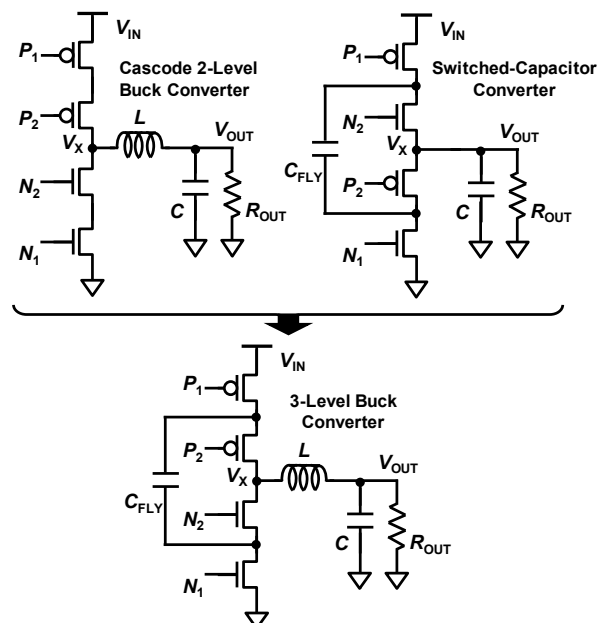


Fig. 1. Power stage and output filters of cascade 2-level buck converter, 1/2 switched capacitor DC-DC converter, and 3-level buck converter.

function of 3-level buck converters in the DCM are derived for the first time, enabling the design of controllers. In Section II, the circuit operation of 3-level buck converters in the DCM is shown. A detailed derivation of circuit characteristics including the transfer function in the DCM is given in Section III, and in Section IV, a time-domain small-signal-injection simulation validates the derived results. Finally, Section V concludes this paper.

II. CIRCUIT OPERATION OF 3-LEVEL BUCK CONVERTERS IN DISCONTINUOUS CONDUCTION MODE

The 3-level buck converter in Fig. 1 includes four switches (P_1 , P_2 , N_1 , and N_2). As shown in Fig. 2, the 3-level buck converter in the DCM has 5 states (S_1 – S_5), instead of the 4 states (S_1 – S_4) in the 3-level buck converter in the CCM [3]. S_5 only exists in the DCM and the inductor current (I_L) is zero in the S_5 state. Fig. 3 shows operation waveforms of the voltage in the V_X node and I_L in the 3-level buck converter in the DCM. T_S is the duration of one period and D_1 – D_6 are duty ratios. D_1 , D_2 , and D_3 are assumed to be equal to D_4 , D_5 , and D_6 , respectively. Note that the voltage across the flying capacitor (V_{FLY}) is assumed to be half of V_{IN} in the case of a sufficiently large C_{FLY} . When the conversion ratio M ($= V_{OUT}/V_{IN}$) is less than 1/2, the state transition order is (S_1 , S_2 , S_5 , S_3 , S_2 , S_5). In contrast, when M is above 1/2, the order is (S_4 , S_1 , S_5 , S_4 , S_3 , S_5).

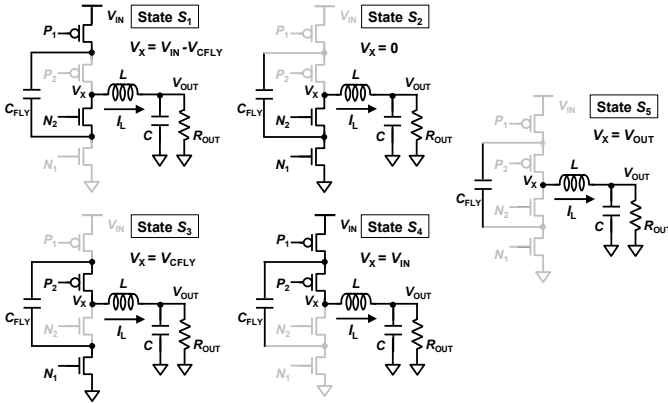


Fig. 2. Five circuit states of 3-level buck converters (S_1 - S_5).

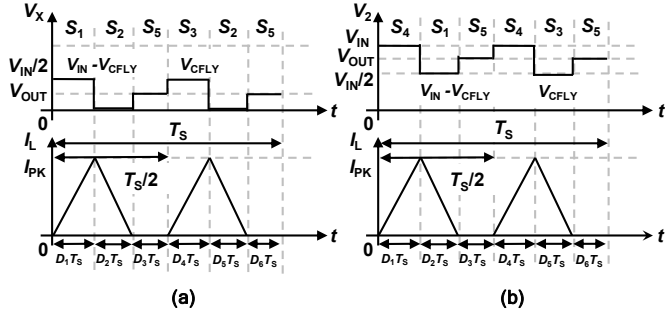


Fig. 3. Switching patterns of 3-level buck converter. (a) $M \leq 0.5$, (b) $M \geq 0.5$.

III. CIRCUIT CHARACTERISTICS OF 3-LEVEL BUCK CONVERTERS IN DISCONTINUOUS CONDUCTION MODE

A. Analysis of Conversion Ratio

The conversion ratio M of a 3-level buck converter in the DCM is derived by combining the volt-second balance in the inductor voltage (V_L), and the balance of the load current and the averaged I_L .

$$\langle V_L \rangle = 0 \quad (1)$$

$$\frac{V_{OUT}}{R_{OUT}} = \langle I_L \rangle \quad (2)$$

When $M \leq 0.5$, (1) is expressed as

$$\begin{aligned} 0 &= (V_{IN} - V_{CF} - V_{OUT})D_1T_s + (0 - V_{OUT})D_2T_s + 0 \cdot D_3T_s \\ &\quad + (V_{CF} - V_{OUT})D_4T_s + (0 - V_{OUT})D_5T_s + 0 \cdot D_6T_s \end{aligned} \quad (3)$$

$$\Leftrightarrow \frac{V_{OUT}}{V_{IN}} = \frac{1}{2} \times \frac{D_1}{D_1 + D_2},$$

and (2) becomes

$$\begin{aligned} \frac{V_{OUT}}{R_{OUT}} &= \frac{1}{2} I_{PK} (D_1 + D_2) \times 2 \\ &= \frac{1}{2} \frac{V_{IN} - V_{OUT}}{L} D_1 (D_1 + D_2) T_s. \end{aligned} \quad (4)$$

By pairing (3) and (4), a quadratic equation for M is acquired,

$$0 = M^2 + \frac{D_1^2}{K} M - \frac{D_1^2}{2K}, \quad (5)$$

where K is defined as

$$K = \frac{2L}{R_{OUT}T_s}. \quad (6)$$

By solving (6), taking the positive sign, M is derived as

$$M = \frac{1}{1 + \sqrt{1 + 2 \left(\frac{K}{D_1^2} \right)}}. \quad (7)$$

When $M \geq 0.5$, (3)–(5), and (7) correspond to (8)–(11), respectively.

$$\frac{V_{OUT}}{V_{IN}} = \frac{D_1 + (D_1 + D_2)}{2(D_1 + D_2)} \quad (8)$$

$$\frac{V_{OUT}}{V_{IN}} = \left(1 - \frac{V_{OUT}}{V_{IN}} \right) \frac{R_{OUT}T_s}{L} D_1 (D_1 + D_2) \quad (9)$$

$$0 = M^2 - \frac{1}{2} \left(1 - \frac{2D_1^2}{K} \right) M - \frac{D_1^2}{K} \quad (10)$$

$$M = \frac{2}{1 - \frac{K}{2D_1^2} + \sqrt{\left(1 - \frac{K}{2D_1^2} \right)^2 + \frac{4K}{D_1^2}}} \quad (11)$$

Note that (7) and (11) are expressed in terms of only the control parameter D_1 and circuit parameters such as L , T_s , and R_{OUT} .

B. Analysis of Transfer Function with Averaged Switch Model

The transfer functions of a 3-level buck converter in the DCM are derived by using an averaged switch model of switch networks [8]. Fig. 4 shows the switch network in a 3-level buck converter in the DCM. The voltage and current waveforms corresponding to Fig. 4 are illustrated in Fig. 5. The averaged switch network quantities, $\langle V_1 \rangle$, $\langle V_2 \rangle$, $\langle I_1 \rangle$, and $\langle I_2 \rangle$, are calculated as follows: When $M \leq 0.5$,

$$\begin{cases} \langle V_1 \rangle = V_{IN} \\ \langle V_2 \rangle = V_{OUT} \\ \langle I_1 \rangle = \frac{D_1^2 T_s}{2L} \left(\frac{V_{IN} - V_{OUT}}{2} \right) \\ \langle I_2 \rangle = \frac{D_1^2 T_s}{2L} \cdot \frac{V_{IN}}{V_{OUT}} \left(\frac{V_{IN} - V_{OUT}}{2} \right), \end{cases} \quad (12)$$

and when $M \geq 0.5$,

$$\begin{cases} \langle V_1 \rangle = V_{IN} \\ \langle V_2 \rangle = V_{OUT} \\ \langle I_1 \rangle = \frac{D_1^2 T_s}{L} \frac{V_{OUT} (V_{IN} - V_{OUT})}{2V_{OUT} - V_{IN}} \\ \langle I_2 \rangle = \frac{D_1^2 T_s}{L} \frac{V_{IN} (V_{IN} - V_{OUT})}{2V_{OUT} - V_{IN}}. \end{cases} \quad (13)$$

Fig. 6 shows the small-signal equivalent circuit of Fig. 4. For small signals, the equivalent circuit is obtained by linearization of the expressions for the averaged switch models. Note that v_1 , v_2 , i_1 , i_2 , and d are small perturbations from $\langle V_1 \rangle$, $\langle V_2 \rangle$, $\langle I_1 \rangle$, $\langle I_2 \rangle$, and D_1 , respectively. The parameters (j_1 , g_1 , r_1 , j_2 , g_2 , and r_2) in Fig. 6 are summarized in Table I.

From the small-signal equivalent model, a control-to-output transfer function can be found as follows:

$$G_{vd}(s) = \frac{v_{OUT}}{d} \Big|_{v_{IN}=0} = \frac{G_{d0}}{1 + s/\omega_p} \quad (14)$$

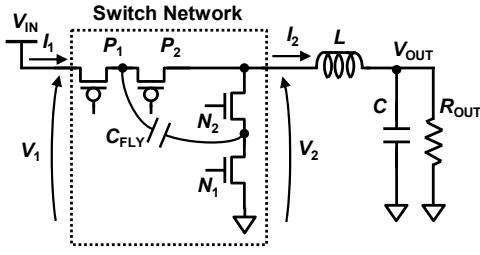


Fig. 4. 3-level buck converter with definition of switch network terminal quantities, V_1 , V_2 , I_1 , and I_2 .

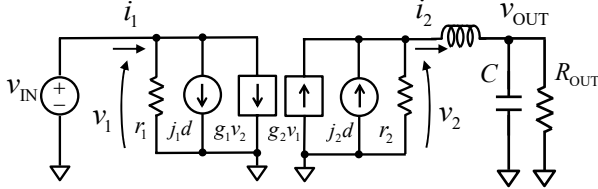


Fig. 6. Small-signal ac models of 3-level buck converter in DCM obtained by averaged switch model.

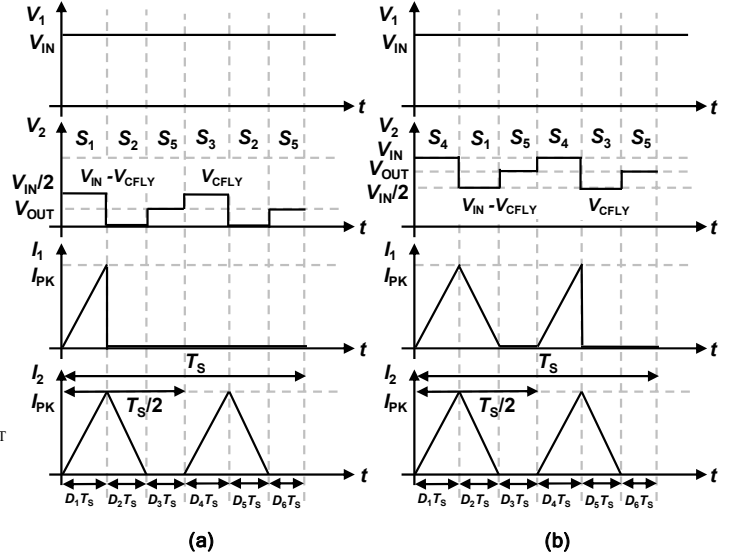


Fig. 5. Voltage and current waveforms of switch network. (a) $M \leq 0.5$, (b) $M \geq 0.5$.

Table I. Summary of parameters in Fig. 6

3-Level Buck Converter	$j_1 \equiv \frac{\partial \langle i_1 \rangle}{\partial D_1}$	$r_1 \equiv 1 / \frac{\partial \langle i_1 \rangle}{\partial V_{IN}}$	$g_1 \equiv - \frac{\partial \langle i_1 \rangle}{\partial V_{OUT}}$	$j_2 \equiv \frac{\partial \langle i_2 \rangle}{\partial D_1}$	$r_2 \equiv -1 / \frac{\partial \langle i_2 \rangle}{\partial V_{OUT}}$	$g_2 \equiv \frac{\partial \langle i_2 \rangle}{\partial V_{IN}}$
$0 \leq M \leq 0.5$	$j_1 = \frac{2D_1V_{IN}}{KR_{OUT}} \left(\frac{1}{2} - M \right)$	$r_1 = \frac{2KR_{OUT}}{D_1^2}$	$g_1 = \frac{D_1^2}{KR_{OUT}}$	$j_2 = \frac{D_1V_{IN}}{KR_{OUT}} \cdot \frac{1-2M}{M}$	$r_2 = \frac{2KR_{OUT}}{D_1^2} M^2$	$g_2 = \frac{D_1^2}{KR_{OUT}} \cdot \frac{1-M}{M}$
$0.5 \leq M \leq 1.0$	$j_1 = \frac{2D_1V_{IN}}{KR_{OUT}} \cdot \frac{2M(1-M)}{2M-1}$	$r_1 = \frac{KR_{OUT}}{2D_1^2} \cdot \frac{(2M-1)^2}{M^2}$	$g_1 = \frac{D_1^2}{KR_{OUT}} \cdot \frac{(2M-1)^2 + 1}{(2M-1)^2}$	$j_2 = \frac{2D_1V_{IN}}{KR_{OUT}} \cdot \frac{2(1-M)}{2M-1}$	$r_2 = \frac{KR_{OUT}}{2D_1^2} (2M-1)^2$	$g_2 = \frac{2D_1^2}{KR_{OUT}} \cdot \frac{1-2(M-1)^2}{(2M-1)^2}$

Table II. Values of M and control-to-output transfer function $G_{vd}(s)$ of 2-level and 3-level buck converters in DCM

	2-Level DCM Buck Converter [8]	3-Level DCM Buck Converter (This Work)	
		$M < 0.5$	$M > 0.5$
$M = V_{OUT}/V_{IN}$	$\frac{2}{1 + \sqrt{1 + 4 \left(\frac{K}{D_1^2} \right)}}$	$\frac{1}{1 + \sqrt{1 + 2 \left(\frac{K}{D_1^2} \right)}}$	$\frac{2}{1 - \frac{K}{2D_1^2} + \sqrt{\left(1 - \frac{K}{2D_1^2} \right)^2 + \frac{4K}{D_1^2}}}$
$G_{vd}(s)$	$G_{d0} / \left(1 + \frac{s}{\omega_p} \right)$		
G_{d0}	$\frac{MV_{IN}}{D_1} \cdot \frac{2(1-M)}{2-M}$	$\frac{MV_{IN}}{D_1} \cdot \frac{1-2M}{1-M}$	$\frac{MV_{IN}}{D_1} \cdot \frac{2(1-M)(2M-1)}{1-2(M-1)^2}$
ω_p	$\frac{1}{R_{OUT}C} \cdot \frac{2-M}{1-M}$	$\frac{1}{R_{OUT}C} \cdot \frac{2(1-M)}{1-2M}$	$\frac{1}{R_{OUT}C} \cdot \frac{1-2(M-1)^2}{(2M-1)(1-M)}$

Table III. Values of M and control-to-output transfer function $G_{vd}(s)$ of 2-level and 3-level buck converters in CCM

	2-Level CCM Buck Converter [9]	3-Level CCM Buck Converter [5,6]	
		$M < 0.5$	$M > 0.5$
$M = \frac{V_{OUT}}{V_{IN}}$	D	D_1	$D_1 + \frac{1}{2}$
$G_{vd}(s)$	$G_{d0} / \left(1 + \frac{s}{Q\omega_0} + \frac{s^2}{\omega_0^2} \right)$		
G_{d0}	V_{IN}		
ω_0	$\frac{1}{\sqrt{LC}}$		
Q	$R_{OUT} \sqrt{\frac{C}{L}}$		

$$G_{d0} = j_2 (R_{OUT} \parallel r_2) \quad (15)$$

$$\omega_p = \frac{1}{(R_{OUT} \parallel r_2)C} \quad (16)$$

Note that in the equivalent circuit, the inductor is in series with the input current source; thus, the inductor dynamics

(particularly at low frequencies) is assumed insignificant [8]. In Table II, values of M and the control-to-output transfer function of the 2-level [8] and 3-level buck converters in the DCM are summarized. For comparison, Table III shows values of M and the transfer function of the 2-level [9] and 3-level [5-6] buck converters in the CCM. Similar to conventional 2-level buck

converters, 3-level buck converters in the DCM have a first-order lag transfer function, while 3-level buck converters in the CCM have a second-order lag transfer function, suggesting that different controllers are required for the DCM and CCM. In the design of a conventional 2-level buck converter operating both in the CCM for heavy loads (e.g., 100mA) in the active mode and in the DCM for light loads (e.g., 0.1mA) in the stand-by mode, the controller must be carefully designed for combined operation in the CCM and DCM [10]. The proposed model enables the design of controllers for 3-level buck converters in the DCM.

IV. VALIDATION OF DERIVED TRANSFER FUNCTION BY TIME-DOMAIN SMALL-SIGNAL-INJECTION SIMULATION

The derived transfer function is verified by time-domain small-signal-injection simulation. In the behavioral model of a 3-level buck converter on the MATLAB/Simulink platform, a small-amplitude sinusoidal signal at a given frequency is injected into the input of a PWM modulator. The response of the 3-level buck converter at the frequency is obtained by comparison of the amplitude and phase shift between the input signal and output signal. The orthogonal demodulation scheme is employed to calculate the gain and phase characteristics [11]. Whole-frequency characteristics of the transfer function are acquired by sweeping the frequencies of the injected signals. Since C_{FLY} does not exist in the derived transfer function, an ideal DC voltage of half of V_{IN} is used instead of C_{FLY} . Note that in this case, a negligible ripple voltage on C_{FLY} is assumed. Fig. 7 shows Bode plots of the derived transfer function in Table II and simulation results under the conditions of $f_{sw}=50\text{MHz}$, $L=56\text{nH}$, $C=10\text{nF}$, $R_{OUT}=30\Omega$, $V_{IN}=5\text{V}$, $D_1=0.25\text{V}$, $M=0.275$. The Bode plot of the derived transfer function is consistent with that of the simulated results, which indicates the validity of the derived transfer function of the 3-level buck converter in the DCM.

V. CONCLUSION

In this paper, the modeling of 3-level buck converters in the DCM was conducted. The transfer function was derived by using an averaged switch model and verified by time-domain small-signal-injection simulation. It was revealed that 3-level buck converters in the DCM have a first-order lag transfer function, while 3-level buck converters in the CCM have a second-order lag transfer function, suggesting that different controllers are required for the DCM and CCM, similar to conventional 2-level buck converters.

REFERENCES

[1] W. Kim, D. Brooks, and G.-Y. Wei, "A fully-integrated 3-level DC-DC converter for nanosecond-scale DVFS," *IEEE J. Solid-State Circuits*, vol. 47, no. 1, pp. 206–219, Jan. 2012.

[2] P. Kumar, V. A. Vaidya, H. Krishnamurthy, S. Kim, G. E. Matthew, S. Weng, B. Thiruvengadam, W. Proefrock, K. Ravichandran, and V. De, "A 0.4V–1V 0.2A/mm² 70% efficient 500 MHz fully integrated digitally controlled 3-level buck voltage regulator with on-die high density MIM capacitor in 22nm tri-gate CMOS," in *Proc. IEEE Custom Integrated Circuits Conf.*, Sept. 2015, pp. 1–4.

[3] X. Liu, C. Huang, and P. K. T. Mok, "A 50MHz 5V 3W 90% efficiency 3-level buck converter with real-time calibration and wide output range

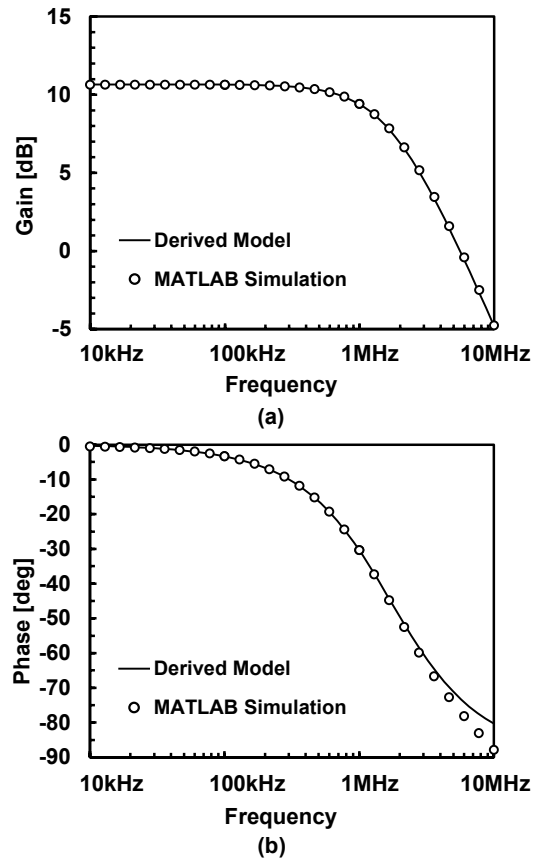


Fig. 7. Bode plots of derived theoretical model and time-domain simulation results of (a) gain and (b) phase under conditions of $f_{sw}=50\text{MHz}$, $L=56\text{nH}$, $C=10\text{nF}$, $R_{OUT}=30\Omega$, $V_{IN}=5\text{V}$, $D_1=0.25$, $M=0.275$.

for fast-DVS in 65nm CMOS," in *Proc. IEEE Symp. VLSI Circuits*, June 2016, pp. 52–53.

[4] G. Villar and E. Alarcon, "Monolithic integration of a 3-level DCM-operated low-floating-capacitor buck converter for DC-DC step-down conversion in standard CMOS," in *Proc. IEEE Power Electron. Specialists Conf.*, Jan. 2008, pp. 4229–4235.

[5] X. Liu, C. Huang, and P.K.T. Mok, "Dynamic performance analysis of 3-level integrated buck converters," in *Proc. IEEE Int. Symp. Circuits Syst.*, May 2015, pp. 2093–2096.

[6] X. Liu, P. K. T. Mok, J. Jiang and W. H. Ki, "Analysis and design considerations of integrated 3-level buck converters," *IEEE Trans. Circuits Syst. I, Reg. Papers*, vol. 63, no. 5, pp. 671–682, May 2016.

[7] N. Kurd, M. Chowdhury, E. Burton, T. P. Thomas, C. Mozak, B. Boswell, M. Lal, A. Deval, J. Douglas, M. Elassal, A. Nalamalpu, T. M. Wilson, M. Merten, S. Chennupati, W. Gomes, and R. Kumar, "Haswell: a family of IA 22nm processors," in *Proc. IEEE Int. Solid State Circuits Conf.*, Feb. 2014, pp. 112–113.

[8] J. Chen, R. Erickson, and D. Maksimovic, "Averaged switch modeling of boundary conduction mode dc-to-dc converters," in *Proc. IEEE IECON*, Nov. 2001, pp. 844–849.

[9] R. Erickson and D. Maksimovic, *Fundamentals of Power Electronics*, 2nd ed., New York, NY, USA: Springer, 2001.

[10] C. H. van der Broeck, R. W. De Doncker, S. A. Richter, and J. v. Bloh, "Unified control of a buck converter for wide-load-range applications," *IEEE Trans. Ind. Appl.*, vol. 51, no. 5, pp. 4061–4071, Sept.–Oct. 2015.

[11] Y. Sugimoto, "A highly efficient transient and frequency-response simulation method for switching converters without using a SPICE-like analog simulator," in *Proc. IEEE Int. Symp. Circuits Syst.*, May 2010, pp. 1308–1311.